



HAL
open science

Spin transfer torque magnetization reversal in a hard/soft composite structures

M Kuteifan, C.-H Lambert, M V Lubarda, V. Lomakin, E. E. Fullerton, S. Mangin

► **To cite this version:**

M Kuteifan, C.-H Lambert, M V Lubarda, V. Lomakin, E. E. Fullerton, et al.. Spin transfer torque magnetization reversal in a hard/soft composite structures. AIP Advances, 2018, 8, pp.015024. 10.1063/1.5009589 . hal-02086009

HAL Id: hal-02086009

<https://hal.univ-lorraine.fr/hal-02086009v1>

Submitted on 1 Apr 2019



HAL is a multi-disciplinary open access archive for the deposit and dissemination of scientific research documents, whether they are published or not. The documents may come from teaching and research institutions in France or abroad, or from public or private research centers.

L'archive ouverte pluridisciplinaire **HAL**, est destinée au dépôt et à la diffusion de documents scientifiques de niveau recherche, publiés ou non, émanant des établissements d'enseignement et de recherche français ou étrangers, des laboratoires publics ou privés.

Spin transfer torque magnetization reversal in a hard/soft composite structures

Cite as: AIP Advances **8**, 015024 (2018); <https://doi.org/10.1063/1.5009589>

Submitted: 17 October 2017 . Accepted: 09 January 2018 . Published Online: 25 January 2018

M. Kuteifan , C.-H. Lambert, M. V. Lubarda, V. Lomakin, E. E. Fullerton, and S. Mangin 



View Online



Export Citation



CrossMark

ARTICLES YOU MAY BE INTERESTED IN

[Estimation of thermal stability factor and intrinsic switching current from switching distributions in spin-transfer-torque devices with out-of-plane magnetic anisotropy](#)

AIP Advances **8**, 015011 (2018); <https://doi.org/10.1063/1.5002139>

[Efficient micromagnetic modelling of spin-transfer torque and spin-orbit torque](#)

AIP Advances **8**, 056008 (2018); <https://doi.org/10.1063/1.5006561>

[Spin-orbit torque-induced switching in ferrimagnetic alloys: Experiments and modeling](#)

Applied Physics Letters **112**, 062401 (2018); <https://doi.org/10.1063/1.5017738>



Don't let your writing keep you from getting published!

AIP | Author Services

Learn more today!



Spin transfer torque magnetization reversal in a hard/soft composite structures

M. Kuteifan,^{1,2,a} C.-H. Lambert,¹ M. V. Lubarda,^{3,2} V. Lomakin,²
E. E. Fullerton,² and S. Mangin^{1,2}

¹*Institut Jean Lamour, UMR CNRS 7198, Université de Lorraine, 54506 Vandoeuvre lès Nancy, France*

²*Center of Memory and Recording Research, University of California, San Diego, California 92093-0401, USA*

³*Faculty of Polytechnics, University of Donja Gorica, Oktoih 1, 81000 Podgorica, Montenegro*

(Received 17 October 2017; accepted 9 January 2018; published online 25 January 2018)

Current induced magnetization manipulation in a spin valve structure where the free layer is a magnetic hard/soft composite structure is studied using micromagnetic simulations. In this structure where the hard layers has strong perpendicular magnetic anisotropy, a domain wall can be nucleated in the soft layer due to the spin transfer torque effect. Depending on the magnetic properties of the layers and the current intensity the domain wall can induce the free layer reversal or be pinned by the hard layer. For these non-uniform magnetic configurations both bulk and interface spin transfer torques need to be considered. The potential reduction of the critical current observed in this geometry is of potential technological interest. © 2018 Author(s). All article content, except where otherwise noted, is licensed under a Creative Commons Attribution (CC BY) license (<http://creativecommons.org/licenses/by/4.0/>). <https://doi.org/10.1063/1.5009589>

It is now well established that due to spin transfer torque (STT), a polarized current can induce magnetization switching or precession. Those effects are promising technologies for two different application STT-MRAM (magnetic random access memories) and STT-NO (nano-oscillators). One of the present challenges to implement STT-MRAM lies on the reduction of the critical current whereas STT-NO depends on the maximum output power and the narrower frequency bandwidth of the oscillations possible. To improve these two technologies many studies have been performed to find optimal materials and geometries. For instance perpendicular magnetic anisotropy (PMA) materials have shown to improve both switching current for STT-MRAM^{1,2} and the output power for STT-NO.^{3,4} However up to now, most of the studies have considered free layers with uniform magnetization.

More complex structures like hard/soft magnetic bilayers were studied for their interesting magnetic properties^{5,6} and magnetic recording performance.^{7–10} In this case using an external magnetic field and depending on the bilayer structure a domain wall nucleated in the soft layer can be pinned or propagate through the hard layer. If pinned the domain wall can then be compressed on the energy barrier created by the hard layer.⁶ For applications, it was shown using a macrospin model that such structures could provide a lower switching field for a given thermal stability.¹¹

In this Letter, we are studying the effect of spin transfer torque on a perpendicular hard/soft structure. Our goal is to answer basic questions such as can a domain wall be nucleated, pinned, and compressed by a polarised current as it is possible with a magnetic field? Do we have to consider both interface and bulk spin transfer torques? As well as more technology related questions such as how is the switching current affected by the hard/soft structure?

^aemail: makuteif@eng.ucsd.edu



We used the FastMag micromagnetics code¹² to simulate the behaviour of a spin valve containing a hard/soft composite free layer under an applied polarized current. The z axis is defined as the direction along the magneto-crystalline anisotropy axis, perpendicular to the film plan. Current is regarded as positive when electrons are flowing in the $+z$ direction.

The first sample geometry considered is a pillar structure with a $5 \times 5 \text{ nm}^2$ section. Its magnetic structure is divided in two blocks: a 5nm-thick polarizer (reference layer) and a 7 to 20 nm-thick composite free layer, separated from each other by a 1 nm non-magnetic spacer. The reference and free layers are considered fully decoupled with respect to the exchange interaction, which allows us to focus on the influence of the polarized current flowing through the composite free layer. All layers have PMA along the z axis. The composite free layer is made of a soft and hard sublayer having respectively a uniaxial magnetic anisotropy constants $K_S = 1.5 \times 10^4 \text{ erg/cm}^3$ and $K_H = 1.5 \times 10^7 \text{ erg/cm}^3$, and a saturation magnetization $M_S = 800 \text{ emu/cm}^3$ and $M_H = 200 \text{ emu/cm}^3$, respectively. The damping parameter was chosen to be $\alpha=0.05$. The initial magnetization of the reference layer and the free layer are along $-z$ and $+z$ directions, correspondingly.

The micromagnetic simulations are based on the solution of the Landau-Lifshitz-Gilbert-Slonczewsky (LLGS) equation modified to take into account the effect of both the spin-transfer torque in the bulk¹³ as well as the spin-transfer torque at the interface.¹⁴ The LLGS equation is written as:

$$\frac{\partial \mathbf{M}}{\partial t} = \gamma (\mathbf{H}_{\text{eff}} + \mathbf{H}_{\text{stt}}) \times \mathbf{M} + \frac{\alpha}{M_S} \mathbf{M} \times \frac{\partial \mathbf{M}}{\partial t} - u \frac{\partial \mathbf{M}}{\partial z} + \frac{\beta u}{M_S} \mathbf{M} \times \frac{\partial \mathbf{M}}{\partial z}$$

where \mathbf{M} is the magnetization, γ is the gyromagnetic ratio, \mathbf{H}_{eff} is the effective field derived from the energy functional, \mathbf{H}_{stt} is the field derived from the Slonczewsky formulation for interfacial STT effects, α is the damping parameter, M_S is the saturation magnetization, β is the non-adiabatic spin-transfer parameter. The parameter u depends on the current density J and is defined as $u = gJ\mu_B p_B / (2eM_S)$, where g is the Landé factor, μ_B is the Bohr magneton, e is the electron charge, and p_b is the polarization factor of the current in the bulk of the material. The interfacial STT field is written as $\mathbf{H}_{\text{stt}} = jp_i \hbar / (2etM_S) \mathbf{M} \times \mathbf{p}$ where p_i is the polarization factor of the current at the interface, \hbar is the reduced Planck constant, t is the effective thickness related to the mesh size¹⁴ and \mathbf{p} is the magnetization of the reference layer. The finite elements simulations were done using a cell size of 1 nm.

For purposes of later comparison, we first consider the magnetization response of a 15-nm-thick soft layer and a 5-nm-thick hard layer under the influence of an external magnetic field and in the absence of current through the stack. Figure 1 shows that an external field applied to this structure can lead to a DW nucleation in the free layer, compression of the DW when the field is increased, represented by the fact that the average z component of magnetization gets lower, and eventually its propagation through the hard layer when the field becomes strong enough. All these observations are in accordance with typical calculations involving applied magnetic fields.^{6,15}

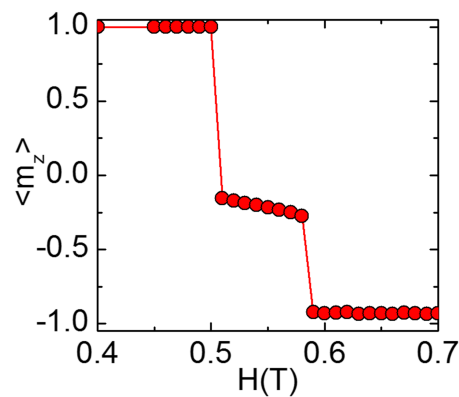


FIG. 1. Average of the z component of the magnetization in the $5 \times 5 \times 20 \text{ nm}^3$ composite free layer as a function of a field applied along the z axis, in the absence of current.

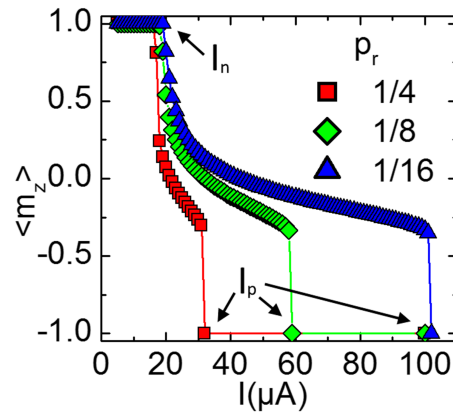


FIG. 2. Average of the z component of the magnetization in the $5 \times 5 \times 20 \text{ nm}^3$ composite free layer as a function of applied current for different polarization ratios p_r .

Figure 2 shows that similarly to an applied field, current can lead to DW nucleation, compression and propagation⁶ owing to spin transfer torque. Since the magnetization along the thickness of the free layer is not uniform, continuous spin transfer torque within this layer has to be accounted for in the calculations. In our model, the interfacial and bulk contributions to the spin transfer torque are modulated separately by introducing an efficiency coefficients for the STT in the bulk of the layers and for STT at the interface. Two distinct STT polarizations, therefore, appear in the model: p_i for the interfacial STT and p_b for the bulk STT. The relative efficiency of bulk STT with respect to interfacial STT we represent using the ratio $p_r = p_b/p_i$. For these cases p_i was chosen to be 1. The physical behaviour of the DW is qualitatively similar for various values of p_r . However this parameter can be tuned to adapt the device to adequate values of applied current depending on different technology and materials.

From the reversal curves in Fig. 2, two characteristic current values can be extracted: the nucleation current I_n that corresponds to the minimum current required to nucleate a domain wall in the structure corresponding to $\langle m_z \rangle < 1$, and the propagation current I_p that indicates the complete reversal of the free layer. Between the two stages, the pillar is in a current-sustained state which exhibits a domain wall in the soft part of the free layer. The bulk STT tends to push the DW towards the hard layer and compress it, while the exchange interaction opposes this compression. Similarly to what happens under an applied field, DW compression becomes greater when the current (and hence bulk STT) is increased. The bulk STT, therefore, has a large impact on I_p where larger values of p_r will lead to reversal at less current.

Figure 3 highlights the influence of the soft sublayer thickness t_S on I_n and I_p for two values of p_r while keeping the hard sublayer thickness constant to 5 nm. Increasing the soft layer thickness from a small value strongly decreases I_n and I_p as the switching is facilitated. For $t_S > 10 \text{ nm}$, I_n becomes relatively stable. The nucleation of a tilt in the free layer essentially comes from the interfacial spin transfer interaction with the reference layer, hence the small difference between $p_r = 1/4$ and $p_r = 1/8$. On the other hand, I_p strongly depends on bulk STT to push the domain wall through the hard sublayer. For this reason I_p is greatly reduced for $p_r = 1/4$. We can observe that I_p saturates for large enough values of t_S . This is explained by the fact that once a domain wall is fully nucleated, it can be pushed through an arbitrarily long distance by bulk STT in an ideal case with no defect.

In the case of magnetic field-driven reversal, composite structures can improve the efficiency of the switching process.^{15–20} Calculations were performed in order to investigate the role of hard and soft thicknesses on optimization of switching current and thermal stability of such systems. The model involves a 7-nm-thick free layer with t_S ranging from 0 to 7 nm and $t_H = 7 \text{ nm} - t_S$. The cross sectional area of the stack is $5 \times 5 \text{ nm}^2$ and the reference layer is 3-nm thick. The anisotropies for the hard and soft layers being used are $K_H = 1.5 \times 10^7 \text{ erg/cm}^3$ and $K_S = 1.5 \times 10^6 \text{ erg/cm}^3$, respectively. The anisotropy of the reference layer is $K_R = 1.0 \times 10^8 \text{ erg/cm}^3$. The saturation magnetization of the

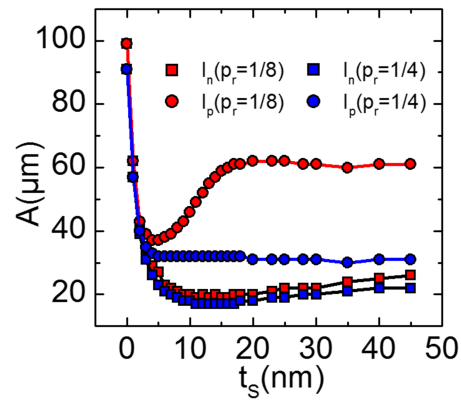


FIG. 3. Evolution of the nucleation current I_n and the propagation current I_p depending on the soft sublayer thickness for two values of the polarization ratio p_r . The cross section is $5 \times 5 \text{ nm}^2$ and the hard sublayer thickness is 5 nm.

free and reference layer are 800 emu/cc and 200 emu/cc, respectively. The damping parameters were chosen to be $\alpha_f=0.02$ for the free layer and $\alpha_r=1$ for the reference layer.

For each structure corresponding to the different values of t_s , the thermal stability was calculated by the nudged-elastic-band (NEB) method using FastMag simulator.^{12,21} This method finds the minimum energy path between the initial (free layer up) and final (free layer down) states of the stack, from which we obtain the energy barrier ΔE (Fig. 4a). This barrier gives the thermal stability of the system. It corresponds to the minimum amount of thermal energy required to switch the free

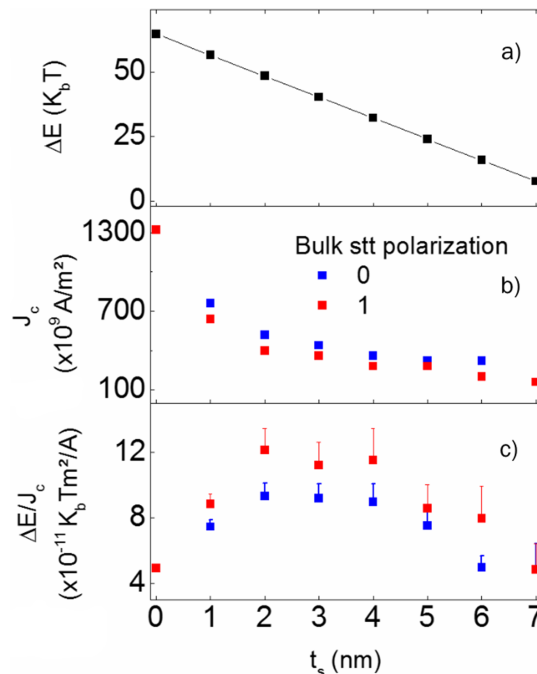


FIG. 4. (a) Energy barrier ΔE of the minimum energy path for the reversal of the composite free layer as a function of soft layer thickness. (b) Critical current density J_c for reversal of the free layer as a function of soft layer thickness for a bulk stt polarization of 0 and 1. (c) switching efficiency defined as $\Delta E/J_c$. Figures obtained for the case of a $5 \times 5 \times 7 \text{ nm}^3$ free layer.

layer. The mode of thermally driven reversal for the modelled structures is uniform rotation of the magnetization, and ΔE decreases linearly with t_S , as expected.

The critical current density for switching J_c was obtained by solving the LLG equation for two cases: in one case, the bulk STT polarization was set to 1, and in the other case, it was ignored (polarization set to 0). In both cases the interfacial STT polarization was set to 1. Comparison of the two cases will highlight the effect of the bulk STT on the reversal process.

For $t_S = 0$ or $t_S = 7$ (completely hard or completely soft free layer) there is no magnetization gradient along the thickness during the reversal of the layer. For this reason the bulk STT has no effect on this process and the critical current densities are identical for the two cases considered. For intermediate values of t_S , nonuniformities of magnetization can develop, due to the interface between the soft and hard layers. In these cases, bulk STT helps the magnetization configuration of the free layer to propagate into the hard layer, making it easier to switch. As a result, J_c is smaller when the bulk STT polarization is 1 instead of 0 (Fig. 4b). Figure 4c shows $\Delta E/J_c$ as a function of t_S . This ratio is commonly regarded as the switching efficiency:²² a high value indicates a device less effected by the trade-off between thermal stability and critical current necessary for switching (power consumption). For both considered polarization values, it is shown that there is a peak in switching efficiency for t_S between 2 and 4 nm. The efficiency is greater when bulk STT is taken into account. This can be explained by looking at the reversal mechanism. The polarizer is interfaced with the soft part of the free layer, where the electrons induce the switching. In these cases the exchange interaction keeps the magnetization uniform through the soft layer, however the difference in anisotropy with the hard layer creates a small angle between both magnetization vectors: it takes longer for the hard layer to switch. When bulk STT is added to the system, the electrons tend to polarize the hard layer (into which they flow) towards the same direction as the soft layer (from which they come), thus effectively helping the switching process.

Hard/soft composite structures with a larger cross sectional area of $50 \times 50 \text{ nm}^2$ have been studied, as well, in order to highlight the effect of lateral size on device characteristics (see Fig. 5). The same

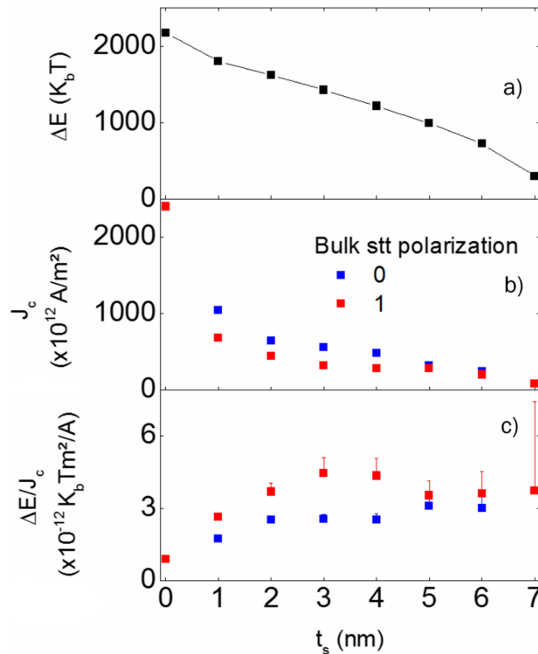


FIG. 5. (a) Energy barrier ΔE of the minimum energy path for the reversal of the composite free layer as a function of soft layer thickness. (b) Critical current density J_c for reversal of the free layer as a function of soft layer thickness for a bulk stt polarization of 0 and 1. (c) Switching efficiency defined as $\Delta E/J_c$. Figures obtained for the case of a $50 \times 50 \times 7 \text{ nm}^3$ free layer.

thickness of 3 nm was kept for the reference layer. The free layer thickness, as in the earlier case was 7 nm, with t_S ranging from 0 to 7 nm and $t_H = 7 - t_S$. The anisotropies for the hard and soft layers were $K_H = 3.0 \times 10^7$ erg/cm³ and $K_S = 3.0 \times 10^6$ erg/cm³, respectively. The anisotropy of the reference layer, saturation magnetization and damping constant were kept the same as the previous case.

The minimum energy paths for the reversal of these structures were calculated by the NEB method as for the smaller model, from which the energy barriers ΔE we obtained (Fig. 5a). Unlike the results for the 5x5-nm² cross-section model, the thermal reversal mode for the larger structures is no longer uniform magnetization rotation, except for $t_s = 7$ nm where the entire free layer is magnetically soft. As soon as the hard sublayer is introduced, the optimal reversal path involves domain wall propagation across the pillar in the lateral direction, as detailed elsewhere.²³ As a consequence, the gain in switching efficiency is much less apparent. When the bulk STT polarization is set to 1, a maximum can be observed for a soft layer thickness around 3 nm. However, the efficiency is only slightly decreased if bulk STT is excluded all together. These results emphasize how the reversal mode, properties of each sublayer, and their interaction can come to bear in the design of devices optimized for low power consumption and high thermal stability.

In conclusion we have shown that composite layers made of sublayers with different anisotropy values can enhance the switching properties under an applied current in order to reduce the critical switching current and keep a good thermal stability. Moreover, the switching threshold and range of domain wall stabilization depend on the bulk spin transfer torque polarization as well as the interfacial spin transfer torque polarization coefficients. The gain in current efficiency in hard/soft structures studied is larger when lateral sizes are smaller and the current-driven reversal is more uniform.

This work was supported by the French Agence Nationale de la Recherche, ANR-10-BLANC-1005 "Friends" by the ANR-NSF Project, ANR-13-IS04-0008-01, "COMAG" by the ANR-Labcom Project LSTNM, by the European Project (OP2M FP7- IOF-2011-298060) and by the Université de la Grande, Institut Carnot ICEEL, the Region Grand Est and Grand Nancy. Work at UCSD supported by the NSF award DMR #1312750.

- ¹ S. Mangin *et al.*, *Nature Mat.* **5**, 210 (2006).
- ² S. Mangin *et al.*, *Appl. Phys. Lett.* **94**, 012502 (2009).
- ³ D. Houssameddine *et al.*, *Nature Materials* **6**(6), 447–453 (2007).
- ⁴ Z. Zhongming *et al.*, *Scientific Reports* **3** (2013).
- ⁵ E. E. Fullerton *et al.*, *Phys. Rev. B* **58**, 00742 (1998).
- ⁶ S. Mangin *et al.*, *Phys. Rev. B* **58**(5), 2748 (1998).
- ⁷ N. F. Supper *et al.*, *IEEE Trans. Magn.* **41**, 3238 (2005).
- ⁸ E. E. Fullerton *et al.*, U.S. patent 7,425,377 (Sept. 16, 2008).
- ⁹ R. H. Victora *et al.*, *IEEE Trans. Magn.* **41**, 2828 (2005).
- ¹⁰ D. Suess *et al.*, *Appl. Phys. Lett.* **87**, 12504 (2005).
- ¹¹ I. Yulaev *et al.*, *Appl. Phys. Lett.* **99**, 132502 (2011).
- ¹² R. Chang *et al.*, *Journal of Applied Physics* **109**(7), 07D358 (2011).
- ¹³ A. Thiaville *et al.*, *Europhys. Lett.* **69**(6), 990–996 (2005).
- ¹⁴ J.-G. Zhu, *IEEE Trans. on Magnetics* **40**(1) (2004).
- ¹⁵ A. Dobin *et al.*, *Appl. Phys. Lett.* **89**, 062512 (2006).
- ¹⁶ D. Goll *et al.*, *Phys. B* **403**, 338–341 (2008).
- ¹⁷ D. Suess, *Appl. Phys. Lett.* **89**, 113105 (2006).
- ¹⁸ S.-S. Yan *et al.*, *J. Mag. Magn. Mat.* **210**, 309–315 (2000).
- ¹⁹ J.-P. Wang *et al.*, *Appl. Phys. Lett.* **86**, 142504 (2005).
- ²⁰ K. Mibu *et al.*, *J. Mag. Magn. Mat.* **163**, 75–79 (1996).
- ²¹ D. Suess *et al.*, *J. Mag. Magn. Mat.* **321**, 545–554 (2009).
- ²² J. Z. Sun *et al.*, *Phys. Rev. B* **88**, 104426 (2013).
- ²³ I. Tudosa, J. A. Katine, S. Mangin, and E. E. Fullerton, *Appl. Phys. Lett.* **96**, 212504 (2010).